# Structure around the Cleavage Site in the Thrombin Receptor Determined by NMR Spectroscopy†

K. John Smith,‡ Ian P. Trayer,‡ and Roger J. A. Grand*,§

*School of Biochemistry and Department of Cancer Studies, University of Birmingham, P.O. Box 363, Edgbaston, Birmingham B15 2TT, U.K.*

*Received December 20, 1993; Revised Manuscript Received March 7, 1994®*

ABSTRACT: NMR spectroscopic experiments were performed to study the structure of synthetic peptides identical to two extracellular regions of the human thrombin receptor. The smaller molecule, comprising 14 amino acids, was biologically active and was equivalent to the "tethered ligand" exposed after cleavage of the receptor by thrombin. The principal structural elements were two overlapping turns (amino acids 5–8 and 6–9), the second of which was stabilized by a hydrogen bond, $6_{CO}$–$9_{NH}$. The five N-terminal residues, considered to be responsible for biological activity, were essentially unstructured. A second version of this peptide, biologically inactive due to the reversal of the two N-terminal amino acids, had a very similar structure. A longer peptide (23 amino acids) covering the proposed thrombin cleavage site was found to be more highly structured. The seven residues from $Pro_{-2}$ to $Arg_5$ (the N-terminal amino acid exposed after cleavage is taken as residue 1) formed a $3_{10}$ helix which is not present in the shorter tethered ligand peptide. The structure is partially stabilized by a charged hydrogen bond between the side chains of $Arg_{-1}$ and $Asp_{-3}$. The overlapping turns observed in the shorter peptides could also be distinguished in the longer molecule. On the basis of the structure determined for the peptide which encompasses the cleavage site and the determined structure of thrombin, a model is postulated for the interaction of the thrombin receptor and the protease during activation.

Thrombin is a serine protease which plays a pivotal role in blood clotting by regulating the conversion of fibrinogen to fibrin. Additionally, it is able to exert an appreciable influence on the behavior of a number of different cell types [reviewed in Shuman (1986)]. For example, it can induce aggregation of platelets (Berndt & Phillips, 1981), chemotaxis in monocytes (Bar-Shavit et al., 1983), and mitogenesis in smooth muscle cells (Chen & Buchanan, 1975). Perhaps more surprisingly, thrombin and prothrombin are capable of regulating neurite outgrowth in cultured primary and immortal neuronal cells (Snider, 1986; Means & Anderson, 1986; Gurwitz & Cunningham, 1988; Grand et al., 1989; Jalink & Moolenaar, 1992; Suidan et al., 1992).

Thrombin interacts with the cells through a specific G protein-coupled receptor which has recently been cloned and sequenced (human sequence: Vu et al., 1991a,b). This protein, of 452 amino acids, is composed of seven transmembrane domains with extra- and intracellular N- and C-terminal domains, respectively. The amino-terminal region comprises approximately 100 amino acids and contains a thrombin cleavage site between residues 41 (arginine) and 42 (serine) as well as an adjacent proposed thrombin-binding domain. It has been suggested, on the basis of homology between this latter region and the thrombin-binding polypeptide hirudin, that it interacts with the anion-binding exo site of thrombin, giving recognition sequences both N-terminal and C-terminal to the cleavage site. Proteolysis of the extracellular domain of the receptor leads to unmasking of a new N-terminus which can then function as a "tethered ligand" peptide, probably interacting with an, as yet, unidentified molecule on the cell surface. This, in turn, triggers the cellular response to thrombin.

This model has been confirmed by elegant mutational studies (Vu et al., 1991a,b; Liu et al., 1991) and by the demonstration that small peptides homologous to that region of the protein freshly exposed after cleavage can substitute for thrombin in the generation of cellular responses. Thus, peptides of only five amino acids can produce many, if not quite all, of the effects of the serine protease (Sabo et al., 1992; Vassallo et al., 1992; Scarborough et al., 1992). In longer peptides, substitutions at amino acids C-terminal to position 6 have little effect on the activity. However, most substitutions in the N-terminal five amino acids render the peptides inactive (Van Obberghen-Schilling et al., 1993). The murine, rat, and hamster thrombin receptors have also been cloned (see Table 1) and found to be very similar to the human homologue, particularly in the hexapeptide sequence exposed after thrombin cleavage and therefore responsible for triggering the receptor.

In view of the highly conserved nature of the receptor and the fact that a large number of different cell types appear to respond in a similar way to the mitogenic activity of thrombin [reviewed in Walz et al. (1986)], it is obviously of great importance to understand the precise mechanism by which the receptor is recognized and cleaved by the protease. With this end in view we have undertaken a study of the structure of the extracellular portion of the protein using synthetic peptides corresponding to a 23-residue peptide which spans the thrombin cleavage site and a 14-residue peptide equivalent to the newly formed tethered ligand. It has been shown, using proton NMR spectroscopy, that the region $Pro_{-2}$–$Arg_5$ in the longer peptide adopts a helical conformation. In both of these molecules two turns have been demonstrated covering residues 6–9 and 5–8. In the shorter peptide the five N-terminal amino acids appear to be unstructured. Reversal of the two

† We are most grateful to the Cancer Research Campaign, London (R.J.A.G.), and the Science and Engineering Research Council, U.K. (I.P.T., K.J.S.), for funding.

* Corresponding author (telephone 021-414-4481; FAX 021-414-4486).

‡ School of Biochemistry.

§ Department of Cancer Studies.

® Abstract published in *Advance ACS Abstracts,* April 15, 1994.

0006-2960/94/0433-6063$04.50/0 

N-terminal amino acids in the biologically active tethered ligand peptide results in a loss of activity but has little or no structural consequences. On the basis of the results of these NMR studies a model for the mechanism of activation of the receptor by thrombin is postulated.

## MATERIALS AND METHODS

*Peptide Sequences.* Three synthetic peptides corresponding to portions of the thrombin receptor were used in this study: (1) the sequence 33–55, containing the thrombin cleavage site between Arg and Ser, which are designated as –1 and 1, respectively

| -9 | -8 | -7 | -6 | -5 | -4 | -3 | -2 | -1 | 1 | 2 | 3 | 4 | 5 | 6 |
|---|---|---|---|---|---|---|---|---|---|---|---|---|---|---|
| A | T | N | A | T | L | D | P | R | S | F | L | L | R | N |
| 33 | 34 | 35 | 36 | 37 | 38 | 39 | 40 | 41 | 42 | 43 | 44 | 45 | 46 | 47 |

| 7 | 8 | 9 | 10 | 11 | 12 | 13 | 14 |
|---|---|---|---|---|---|---|---|
| P | N | D | K | Y | E | P | F |
| 48 | 49 | 50 | 51 | 52 | 53 | 54 | 55 |

(2) the receptor sequence 1–14 (thrombin proreceptor 42–55)

| 1 | 2 | 3 | 4 | 5 | 6 | 7 | 8 | 9 | 10 | 11 | 12 | 13 | 14 |
|---|---|---|---|---|---|---|---|---|---|---|---|---|---|
| S | F | L | L | R | N | P | N | D | K | Y | E | P | F |

and (3) the receptor 1–14, with the first two residues reversed

| 1′ | 2′ | 3 | 4 | 5 | 6 | 7 | 8 | 9 | 10 | 11 | 12 | 13 | 14 |
|---|---|---|---|---|---|---|---|---|---|---|---|---|---|
| F | S | L | L | R | N | P | N | D | K | Y | E | P | F |

The peptides were synthesized by standard Fmoc[1]-protected solid-phase methods (Biotech Instruments BT7600, Alta Bioscience, University of Birmingham, U.K.) and purified to homogeneity by reverse-phase HPLC (using a Vydac C18 column, eluted with a gradient of acetonitrile/0.1% TFA). The purified peptides were sequenced to confirm integrity (Applied Biosystems Inc., model AIB 473A), and in each case only one N-terminus was observed to better than 99%. Positive FAB mass spectra confirmed the mass of peptide –9 to 14 as 2679. Having confirmed the chemical integrity of the peptides, we assigned the small additional resonances observed in NMR spectra for residues toward the C-termini of the peptides to minor cis conformations about the proline residues (as indicated by connectivities in NOESY experiments). Elemental analysis (energy dispersive X-ray microanalysis) excluded the possibility of side reactions involving migration of the sulfonyl moiety of the Pmc-arginine elsewhere in the peptide since no sulfur was present in the peptides [e.g., Jaeger et al. (1993)]. The biological activities of the peptides were assessed by their ability to induce neurite retraction in differentiated Ad12E1HER10 cells (Grabham et al., 1988). Peptides 1 and 3 had no effect on the cells, whereas peptide 2 could substitute for thrombin (Grand et al., 1989).

*NMR Spectroscopy.* All $^1$H-NMR experiments were carried out on a Bruker AMX500 using standard phase-sensitive 2D pulse sequences with TPPI quadrature detection in $F_1$. TOCSY experiments used an MLEV-17 mixing pulse of 60-ms duration (10-kHz locking field), ROESY experiments a continuous mixing pulse of 250-ms duration (3.2-kHz locking field), and NOESY experiments both 50- and 200-ms mixing times. In each case a very weak presaturation was applied to the water peak during the relaxation delay (1.5 s) and also during the mixing time for NOESY and ROESY experiments. Two-dimensional experiments were generally acquired with 2K data points in $F_2$, with a sweep width of 5500 Hz and with 448–512 rows in $F_1$. Sixteen transients were acquired for TOCSY and COSY experiments and 80 transients for NOESY and ROESY experiments. Assignments were based on TOCSY, NOESY, ROESY, and COSY experiments using 10 mM solutions of peptide, at pH 5.9, in 95% $H_2O$/5% $D_2O$ (v/v, 285 K), 50% TFE-$d_3$/50% $H_2O$ (v/v, 292 K), and 50% TFE-$d_3$/50% $D_2O$ (v/v, 292 K), and were quite straightforward. On some occasions the unambiguous identity of NOE cross peaks was confirmed by taking advantage of temperature and solvent-dependent shifts between spectra.

The rate of movement of chemical shifts with changes in either pH or temperature was followed by one-dimensional and TOCSY spectra (8 transients and 256 rows) at each experimental point. The temperature dependence of the backbone amide resonances at pH 5.9, in 50% TFE-$d_3$/50% $H_2O$, was determined using five temperature points, 285, 290, 295, 300, and 305 K, and the temperature shift coefficients were determined from the slope of a plot of temperature versus chemical shift, which was in each case linear. The pH dependence of the peptide resonances was determined at 292 K, in 50% TFE-$d_3$/50% $H_2O$, for pH titration points 1.2, 2.2, 2.8, 3.9, 4.8, and 5.9. The p$K_a$ value for the movement of resonances was determined using the program Enzfit (R. J. Leatherbarrow, 1987, Elsevier Biosoft).

Interproton distances were estimated from NOESY experiments by counting the number of rings for each cross peak. Cross peaks were grouped into five classes between short and very weak. Peptide structures were determined using the XPLOR 3.1 program (Brünger, 1992a) using a protocol in which certain atoms of each residues were embedded using the distance geometry routine (similar to the dg_sub_embed protocol; Brünger, 1992b), the remainder of the atoms were placed by template fitting, and then the peptide coordinates were allowed to evolve under the applied NOE distance constraints during a series of simulated annealing steps (similar to the dgsa and refine protocols). From the first 100 original calculated coordinate sets, approximately half were discarded (wrong handedness), and the final structures were produced by minimizing the averaged coordinates produced over the last 4 ps of a 5-ps low-temperature simulated annealing trajectory. At this point virtually all calculated structures had no NOE violations greater than 0.4 Å. Thirty structures were chosen for analysis with the lowest residual energies, for which the sum of NOE violations for any individual structure was less that 2 Å. The identity of acceptors for hydrogen bonds was confirmed by preliminary calculations, prior to introduction into the calculations as a pseudo-NOE constraint.

Modeling of the *initial* complex between thrombin and its receptor was achieved by placing the calculated structures for peptide –9 to 14 into the thrombin substrate cleft. The coordinates for human thrombin were extracted from the preliminary PDB entry P1DWE (Banner & Hadvary, 1992), which is a cocomplex of thrombin with PPACK and a peptide from the C-terminus of hirudin (residues 55–65), with the inhibitors binding at the active site and the anion-binding exo site, respectively (these thrombin coordinates were chosen since the "south" loop $Glu_{146}$–$Lys_{149}E$ is displaced from its original position to that required for the binding of hirudin, as indeed must be the case in the complex with thrombin receptor). A rms translation and rotation followed by a

[1] Abbreviations: Fmoc, 9-fluorenylmethoxycarbonyl; Pmc, 2,2,5,7,8-pentamethylchromansulfonyl; TFE, 2,2,2-trifluoroethanol; PPACK, D-Phe-Pro-Arg chloromethyl ketone; COSY, correlated spectroscopy; NOESY, nuclear Overhauser effect spectroscopy; TOCSY, total correlation spectroscopy; TrNOE, transferred NOESY; ROESY, rotating-frame Overhauser spectroscopy; PDB, protein data bank.

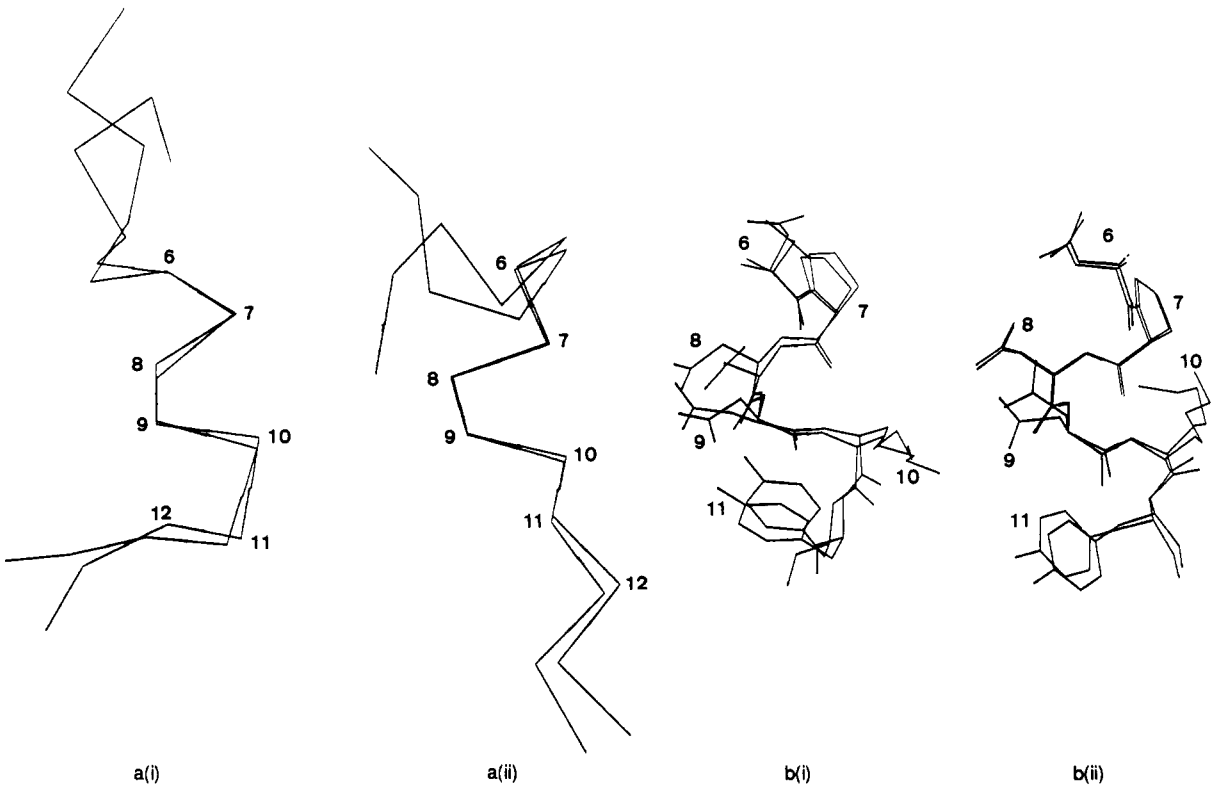


FIGURE 1: Calculated structure of peptide 1–14. Two pairs of overlaid structures for peptide 1–14 are shown. In the two left-hand panels (a) an $\alpha$-carbon trace is shown for the whole peptide, and in the two right-hand panels (b) both backbone and side-chain atoms are illustrated for residues 6–11. Set a(i) and b(i) are views of the same conformation, as are set a(ii) and b(ii). The alignment was made for the given 6–11 in each case. It is clear that there are two alternate conformations which satisfy the observed NOEs, with set (i) corresponding to the more extended conformation at residue $Asn_6$ as described in the text.

simulated annealing protocol were used in XPLOR to place the peptide into the substrate binding cleft, with the $\alpha$-carbon atom positions of the residues $D_{55}FEEI_{59}$ of hirudin and $F_1$-$PR_3$ of PPACK used as target functions for the $\alpha$-carbon coordinates of $K_{10}YEPF_{14}$ and $D_7PR_9$ of peptide –9 to 14, respectively. During these calculations the NOE constraints previously used in calculation of the peptide structures were applied. Structures were chosen in which no additional violations of these constraints were introduced by placement into the cleft (11 conformations). Hydrogen atoms and undefined residues were placed in the crystal coordinates of thrombin in CHARMM (Brooks et al., 1983), and all crystallographically defined non-hydrogen atoms of thrombin were fixed during the dynamics simulations.

Trifluoroethanol was used as a cosolvent with water in this study, because of the well-known ability of TFE/water mixtures to enhance the solution structures of small peptides. This occurs principally by reducing the hydrogen bonding of the peptide amide protons to water and thereby strengthening intramolecular hydrogen bonds and secondary structure (Llinas & Klein, 1985; Nelson & Kallenbach, 1986). Hydrophobic interactions between peptides (aggregation) are also reduced (Lau et al., 1984b). TFE is well-known as a helix-inducing solvent, but it is clear that helices are not induced where no predisposition exists (Dyson et al., 1992; Nelson & Kallenbach, 1989). Other secondary structures stabilized by local hydrogen bonding are also promoted in TFE/water mixtures (for example, $\beta$-turns; Cann et al., 1987; Siligardi et al., 1987), although the interstrand hydrogen bonding of the $\beta$-sheet may not be significantly stabilized in TFE/water mixtures (Buck et al., 1993).

## RESULTS

*Structure of the Region Corresponding to the Thrombin Receptor Sequence 1–14 (Thrombin Proreceptor 42–55).* When the thrombin receptor is activated, it is cleaved by thrombin, and a new N-terminus is revealed which acts as a tethered ligand. The minimal peptide corresponding to the sequence at this new N-terminus which can also activate the thrombin receptor is SFLLR (residues 1–5; Scarborough et al., 1992). $^1$H NOESY and ROESY experiments indicated that the N-terminal segment of peptide 1–14 (residues $Ser_1$ to $Arg_5$) has a poorly defined structure. There are no interresidue contacts observed for either residue $Ser_1$, the aromatic protons of $Phe_2$, or the methyl groups of $Leu_3$, suggesting entirely free rotation of the side chains of these residues. All other interresidue contacts in the region 1–5 are of the type $(i,i+1)$, indicating an ill-defined conformation (not necessarily extended).

The calculated structure for peptide 1–14 is shown in Figure 1. It is clear that, in the region between residues 6 and 14, the peptide adopts a series of $\beta$-turn structures. In $^1$H-NMR $\beta$-turns are identified by some or all of three characteristics (Dyson et al., 1988a): (1) short proton–proton distances detected in NOESY, the most important being the $\alpha$N $(i,i+2)$ connectivity for positions 2 and 4 in the turn; (2) a decrease in the temperature dependence of the amide proton of the residue at position 4 as a result of the formation of a hydrogen bond ($NH_4 \rightarrow CO_1$); and (3) small $^3J_{NH,\alpha H}$ coupling constants for residues at positions 2 and/or 3 of the turn (since coupling constants are averaged in a simple fashion across the whole conformer population, the size of coupling constants may be a good indication of the population of the $\beta$-turn structure). The NOE evidence here indicates three turns which are located by the NOEs, $d_{\alpha N}(i,i+2)$ NOEs for residues $Asn_6$-$Asn_8$, $Pro_7$-$Asp_9$, and $Lys_{10}$-$Glu_{12}$ (the NOEs observed for this peptide are illustrated in Figure 2).

The NOEs defining the 5–8 turn include $d_{\alpha N}(i,i+2)$ and $d_{\beta N}(i,i+2)$ for residues $Asn_6$-$Asn_8$ (see Figure 2). The hydrogen bond $5_{CO}$–$8_{NH}$ is absent, since the amide temperature

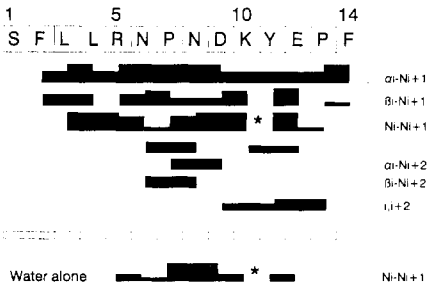


FIGURE 2: NOEs observed for peptide 1–14. An illustration of the sequential and medium-range NOE connectivities for peptide 1–14 in 50% TFE/50% $H_2O$ (v/v), pH 5.9, 292 K, is shown. The thickness of the bars reflects the intensities of the NOEs. The NOE (*) $d_{NN}(i,i+1)$ for residues $Lys_{10}$-$Tyr_{11}$ could not be seen because the amide shifts are too close, placing the NOE very near to the diagonal; the NOEs $d_{NN}(i,i+1)$ for residues $Asp_9$-$Lys_{10}$ and $Tyr_{11}$-$Glu_{12}$ are overlapped in the TFE/water mixture (but not in water). The connectivity $i,i+2$ indicates a class other than $d_{\alpha N}(i,i+2)$ or $d_{\beta N}(i,i+2)$. For proline the $\delta CH_2$ protons substitute for the NH protons. In water (95% $H_2O$/5% $D_2O$ (v/v), pH 5.9, 292 K) the NOE pattern is essentially as seen above, although less intense. In particular, the $d_{\alpha N}(i,i+2)$, $d_{\beta N}(i,i+2)$, and other $i,i+2$ contacts were all present. The lowest panel shows the $d_{NN}(i,i+1)$ connectivities seen in water alone. Note that, for each residue $D_9$ to $F_{14}$, ≈10% of the signal was present at a distinct chemical shift, indicating a second conformation (cis) around the proline residues.

coefficient is high ($8_{NH}$: 8.3 ppb/K), but the NOE is very well defined, so the β-turn is certainly present. Non-hydrogen bonded turns of this type are common in proteins (Richardson & Richardson, 1989) and can be stabilized by side-chain to backbone hydrogen bonding. In the present case, we found a degree of protection of the $Asn_6$ side-chain amide protons from exchange when peptide 1–14, freeze-dried from 50% TFE/$H_2O$, pH 5.9, was redissolved in 50% TFE/$D_2O$ at 290 K. A residual cross peak was present in TOCSY and NOESY spectra after 24 h in solution, indicating that the side chain of $Asn_6$ may hydrogen bond to the carbonyl of residue $Asn_8$ [the NOE $d_{\beta N}(i,i+2)$ for residues $Asn_6$-$Asn_8$ places the side chain pointing into the center of the turn]. For the overlapping turn, 6–9, the expected regular hydrogen-bonding pattern between $6_{CO}$–$9_{NH}$ is seen, with a very low temperature shift coefficient for $9_{NH}$ (1.9 ppb/K). This very low temperature coefficient indicates a high proportion of this turn among the conformers adopted by the peptides, although, surprisingly, as for the other turns described here, there was no obvious reduction in the $^3J_{NH,\alpha H}$ coupling constants. This latter turn can be classified from the Ramachandran plots for the calculated structure of the peptide, which indicate a type I turn at positions 6–9. (A type I turn would be predicted for the sequence 6N-7P-8N-9D, since proline is the most common residue at position 2 and Asn is commonly found in positions 1 and 3.) The Ramachandran plots for residue $Asn_6$ indicate a mixed conformation between an extended and approximately helical conformation, the latter of which would correspond most closely to a type I turn at positions 5–8 [note that the interaction $d_{\text{side chain,NH}}(i,i+2)$ for residues $Asn_6$-$Asn_8$ is compatible with either backbone conformation at residue $Asn_6$]. It is clear that these conformations could exchange in peptide 1–14.

The weak NOE $d_{\alpha N}(i,i+2)$ for residues $Lys_{10}$-$Glu_{12}$ defines a turn at 9–12. In keeping with the size of the NOE, the indication of a hydrogen bond $9_{CO}$–$12_{NH}$ is modest, with a temperature coefficient of only 4.9 ppb/K (4.2 ppb/K for this bond in peptide –9 to 14), and would indicate a much weaker structure and a lower percentage of this turn in the population. Again, the Ramachandran plots of the calculated structures match most closely to a type I turn, although there is considerable variation in the precise backbone conformation observed for both residues $Asp_9$ and $Lys_{10}$. A further turn 10–13 is seen in the calculated structure and arises because weak NOEs between the side chains of residues $Tyr_{11}$ and each of $Asp_9$ and $Pro_{13}$ [$d_{\beta\delta}(i,i+2)$ and $d_{\beta\epsilon}(i,i+2)$ for residues $Asp_9$-$Tyr_{11}$ and $d_{\delta\delta}(i,i+2)$, $d_{\epsilon\delta}(i,i+2)$, $d_{\delta\alpha}(i,i+2)$, $d_{\epsilon\beta}(i,i+2)$, and $d_{\epsilon\gamma}(i,i+2)$ for residues $Tyr_{11}$-$Pro_{13}$] are satisfied simultaneously in the calculation, giving a left-handed twist to the backbone at residue $Glu_{12}$. This may represent the true situation, but the aromatic ring of residue $Tyr_{11}$ may also swing between contacts in a more extended conformation. Of course, there is no amide proton for residue $Pro_{13}$ to form the expected hydrogen bond, so a turn at this position would tend to be less stable.

In addition to the discrete formation of the turns described above, there are indications for a small population of turn-like or helical conformers over the whole range of residues between 5 and 13 of peptide 1–14. In the water/TFE mixture, there are large amide–amide contacts in the NOESY for virtually all residues between 3 and 13, which are all present at reduced mixing times (50 ms) in water/TFE mixtures (and so do not arise from spin diffusion) and are also mostly present in water alone (see Figure 2). These contacts are the most sensitive to a small population of helical $\phi/\psi$ conformations of the peptide backbone (Dyson, 1988a). Confirming this observation, we found a degree of protection of $^1H$ backbone amide protons from $^2H$ exchange (experiment described above). After 24 h in solution there were still small residual cross peaks in TOCSY and NOESY spectra, indicating the presence of unexchanged amide protons for residues $Leu_4$ (very weak), $Arg_5$, $Asn_6$, $Asp_9$, $Lys_{10}$ and $Tyr_{11}$, and $Glu_{12}$. This is a more extensive group than would have been expected from only the turns described above.

*Effect of Reversing the N-Terminal Residues SF to FS in Peptide 1–14.* As mentioned previously, short peptides with the sequence of the new N-terminus of cleaved thrombin receptor are able to activate the receptor. However, when the sequence of the two N-terminal residues is reversed, this ability is lost. We therefore synthesized peptide 1–14 (3) with the residues SF reversed to FS, in order to determine whether there were any structural consequences of this sequence change. Spectra were run under identical conditions for the wild-type and mutant peptides (data not shown), and no significant differences in chemical shifts or NOEs between the two peptides were observed. Since there was no indication of structure for residues 1–5 in the wild-type peptide, then this is also true of the mutant sequence. It is also clear that the change in the sequence of the peptide at the N-terminus has no structural consequences in the C-terminal portion. It is perhaps not too surprising, since biological data indicate that the sequence SFLLR can operate as an independent unit, in that it can mimic most of the functions of the tethered ligand of the thrombin receptor (see introduction), that this region is also independent in terms of conformation from the structural elements toward the C-terminus of peptide 1–14. The implication is that the binding of the sequence SFLLR imposes a structure upon it, in which the sequence SF can contact its binding site. In contrast, the sequence FS must be unable to make the appropriate contacts (Scarborough et al., 1992).

*Structure of the Peptide Corresponding to the Thrombin Receptor Sequence –9 to 14 (Thrombin Proreceptor 33–55).* The conformation of peptide –9 to 14 is illustrated in the observed NOEs (Figure 3) and the calculated structure (Figure 4). The most dramatic feature of the structure is the presence of seven residues in a well-formed helical conformation between $Pro_{-2}$ and $Arg_5$. The presence of a helical conformation with well-ordered side chains is demonstrated by medium-range

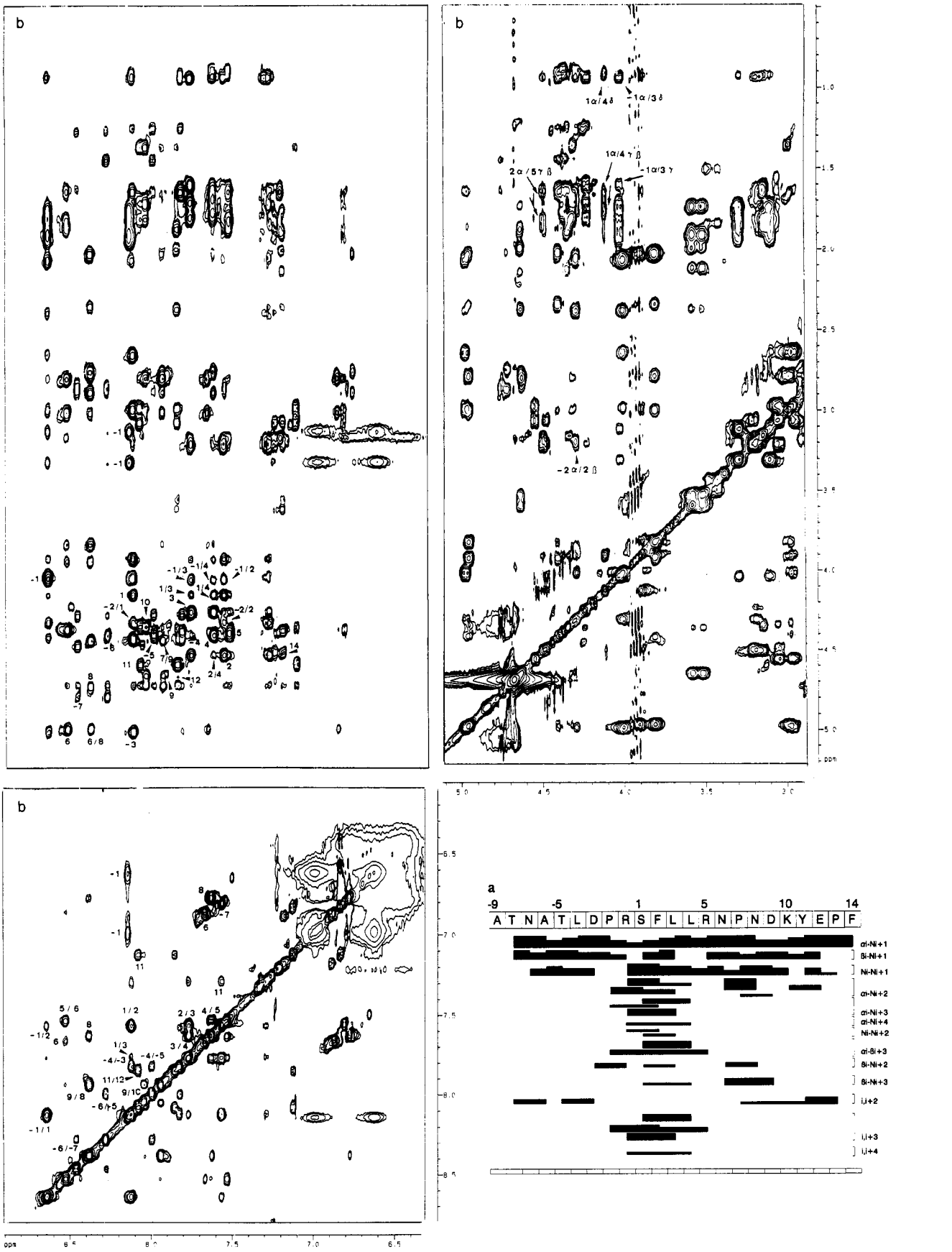


FIGURE 3: NOEs observed for peptide −9 to 14. An illustration of the sequential and medium-range NOE connectivities for peptide −9 to 14 in 50% TFE/50% $H_2O$ (v/v), pH 5.9, 292 K, is shown in panel a. (for key, see figure 2). A composite of a NOESY spectrum (200-ms mixing time) collected under these conditions is shown in panel b. NOEs corresponding to connectivities within a single residue are labeled with a single residue number (−1 refers to an NOE within residue $Arg_{-1}$), while interresidue connectivities are labeled with both residue numbers. In the upper left panel (amide to side-chain and $\alpha$ connectivities) all $d_{\alpha N}(i,i)$ and some long-range $d_{\alpha N}(i,i+1)$ connectivities are labeled (−1/3 refers to the NOE $Arg_{-1,\alpha H}$-$Leu_{3,NH}$). Note also the $d_{\epsilon NH,\delta CH_2}$ connectivities of residue $Arg_{-1}$ (*). All sequential $d_{NN}(i,i+1)$ and some long-range NOEs are labeled in the lower panel. The upper right-hand panel shows the $\alpha$ to side-chain region from a corresponding experiment in 100% $D_2O$.

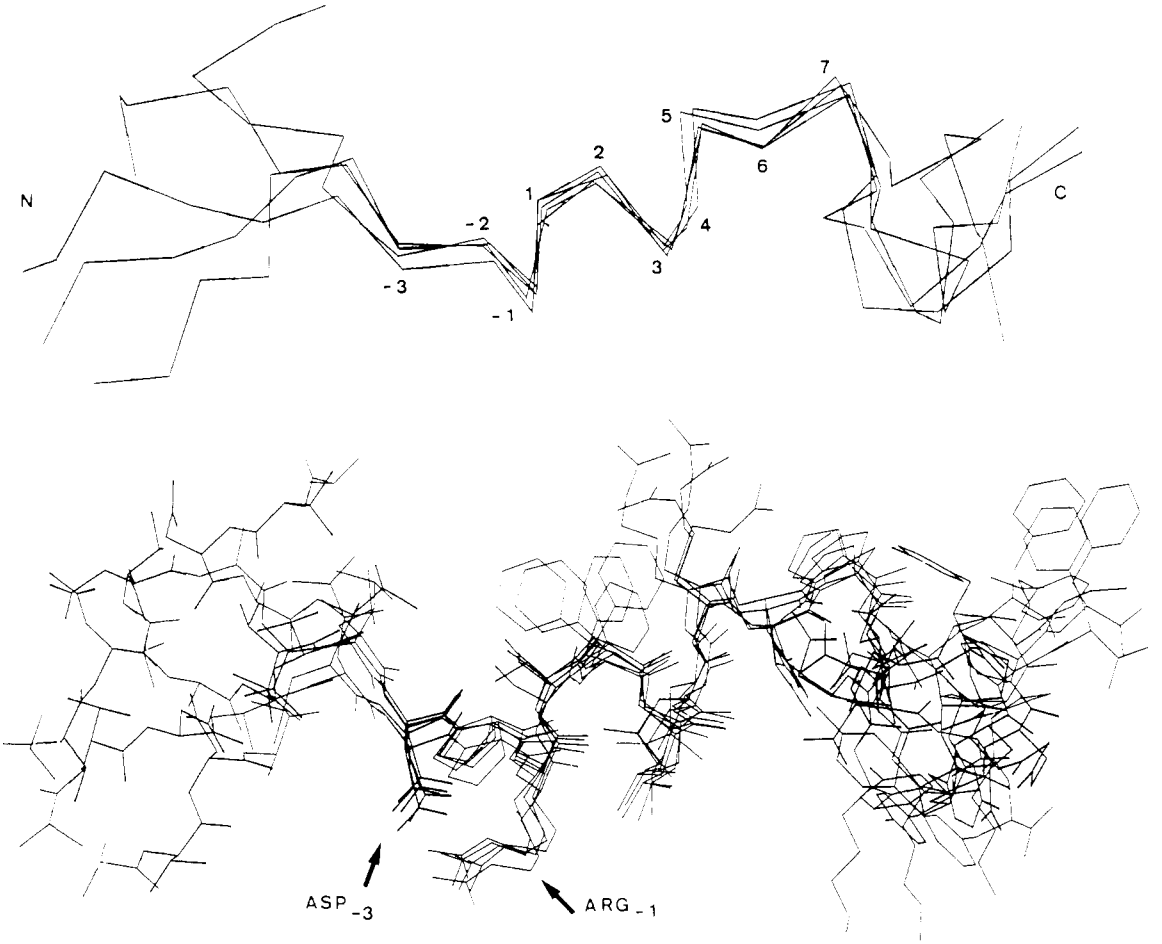


FIGURE 4: Calculated structure of peptide –9 to 14. Five overlaid structures for peptide –9 to 14 are shown. In the upper panel the $\alpha$-carbon atoms only are shown, and in the lower panel both backbone and side chains are included. The alignment was made over the region –4 to +10. The residues $Asp_{-3}$ and $Arg_{-1}$, which are involved in a hydrogen-bonded interaction, are indicated.

connectivities of the type $d_{NN}(i,i+1)$, $d_{\alpha N}(i,i+3)$ ($Pro_{-2}$-$Phe_2$, $Arg_{-1}$-$Leu_3$, $Ser_1$-$Leu_4$), $d_{\alpha\beta}(i,i+3)$ ($Pro_{-2}$-$Phe_2$, $Ser_1$-$Leu_4$, $Phe_2$-$Arg_5$), $d_{\alpha N}(i,i+4)$ ($Arg_{-1}$-$Leu_4$), and $d_{NN}(i,i+2)$ ($Arg_{-1}$-$Phe_2$, $Ser_1$-$Leu_3$). The presence of large NOEs of the type $d_{\alpha N}(i,i+2)$ ($Pro_{-2}$-$Ser_1$, $Arg_{-1}$-$Phe_2$, $Ser_1$-$Leu_3$, $Phe_2$-$Leu_4$) of approximately equivalent size to the corresponding $d_{\alpha N}(i,i+3)$ NOEs identifies the structure in this region as a $3_{10}$ helix, as opposed to the $\alpha$-helix which is more commonly found in peptides. It is conceivable that the structure adopted is a mixture of $\alpha$-helix and $3_{10}$ helix (Karle et al., 1989), with possibly a dynamic exchange of the hydrogen-bonding pattern from the $3_{10}{\equiv}CO_iNH_{i+3}$ to the $\alpha{\equiv}CO_iNH_{i+1}$ (Tirado-Rives & Jorgenson, 1991), but preliminary calculations showed that the NOEs were consistent with a single $3_{10}$ helical conformation, whereas significant violations of the observed NOEs were produced when an $\alpha$-helical hydrogen-bonding pattern was used. The NOE $d_{\alpha N}(i,i+4)$ for residues $Arg_{-1}$-$Leu_4$ is accommodated by a distortion of the regular $3_{10}$ helix in our calculated structure (it is possible that this distortion may reflect averaging in the observed NOEs over $3_{10}$ and $\alpha$-helical conformations). The temperature shift coefficients identify $Phe_2$ and $Arg_5$ amide protons as the principle hydrogen bond donors in this area (coefficients 1.6 and 1.3 ppb/K, respectively), corresponding to a hydrogen-bonding pattern CO ($Pro_{-2}$)–NH($Phe_2$) and CO($Phe_2$)–NH($Arg_5$) in the $3_{10}$ helix. A degree of protection at the amide of $Ser_1$ may be accounted for by a hydrogen bond to the carbonyl of $Asp_{-3}$ (in an Asp-Pro pair at the N-terminus of the helix, the helical hydrogen-bonding pattern frequently extends to the Asp although this residue itself, as here, is in an extended conformation; MacArthur & Thornton, 1991). The protection at the $Arg_{-1}$ amide is certainly due to hydrogen bonding of the side chain oxygen atoms of $Asp_{-3}$ (see below and Figure 6; this type of interaction between the side chain and the amide proton of residues flanking a proline was also described above for $Pro_7$). This side-chain to backbone interaction is common in Asx-Pro-Xxx sequences at the N-terminus of helices in proteins (Richardson & Richardson, 1988). It should be noted that we saw none of the NOE connectivities that would have been expected to arise from the increased ordering of the backbone between residues $Leu_{-4}$ and $Arg_5$ in the more extended hydrogen-bonding network that would have been present in an $\alpha$-helical conformation. Helix formation is cooperative so that the termination of the helix after seven residues must have a specific cause. This appears to lie mainly in the lack of hydrogen bonding to the amide protons of residues $Leu_3$ and $Leu_4$. The temperature shift coefficients, even though quite low, do not change between peptides –9 to 14 and 1–14 (Figure 5). Since one carbonyl acceptor is absent in the shorter peptide, then the low coefficients of the amide protons for residues $Leu_3$ and $Leu_4$ are probably attributable to steric solvent protection by the side chains. In addition, the residue $Pro_7$ would be expected to terminate any residual helix-forming capacity since it lacks an amide proton ($i$) and would disrupt the formation of a hydrogen bond to the ($i$+1) amide proton (Barlow & Thornton, 1988) and the ($i$–1) residue ($Asn_6$) will be sterically hindered to form a $\beta$-conformation (MacArthur & Thornton, 1991).

The N-terminal residues –7 to –4 of the peptide adopt an approximately random extended conformation. In the region 5–14 of peptide –9 to 14, the structure observed is very similar to that described for the shorter peptide in the previous section.

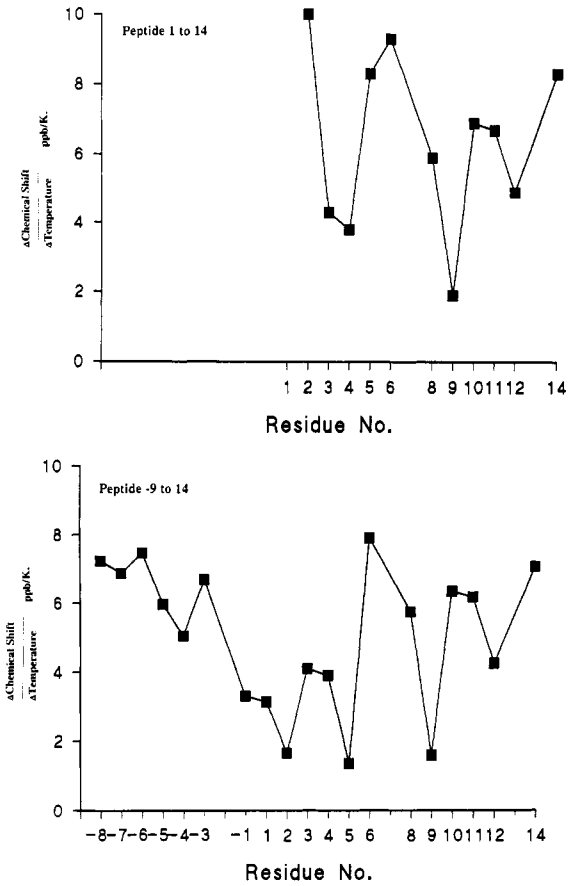


FIGURE 5: Temperature shift coefficients for the backbone amide protons of peptides −9 to 14 and 1–14. The temperature chemical shift coefficients for peptides 1–14 and −9 to 14 plotted against residue number, measured in 50% TFE/50% $H_2O$ (v/v), pH 5.9, between 285 and 305 K, are shown.

The irregular turn 5–8 is still defined by NOEs including $d_{\alpha N}(i,i+2)$ for residues $Asn_6$-$Asn_8$ and still has no indication of a stabilizing hydrogen bond $5_{CO}$–$8_{NH}$ ($8_{NH}$ temperature coefficient 5.7 ppb/K). The backbone at residue $Asn_6$ is now almost exclusively in the $\beta$-conformation (similar to the conformation at $Asp_{-3}$, which is also on the N-terminal side of a proline residue), so that the alternate type I turn conformation described for peptide 1–14 is now excluded. Effectively, the extended conformation around residue $Asn_6$ has been "trapped" in the longer peptide −9 to 14. The turn 6–9 is defined by the NOE $d_{\alpha N}(i,i+2)$ for residues $Pro_7$-$Asp_9$, although this is of reduced magnitude. This does not appear to indicate a change in the strength of the turn at this position since the amide shift coefficient is still very low ($9_{NH}$, 1.6 ppb/K). This principal difference in conformation lies at residue $Asp_9$ and results from the appearance of additional longer range weak NOEs, indicating increased ordering of the side chains [$d_{\beta N}(i,i+3)$ for $Asn_6$-$Asp_9$; $d_{\gamma CH_2,NH}(i,i+2)$ for $Pro_7$-$Asp_9$]. The pH titration experiments provided additional information about the conformation of the peptide in this region. The p$K_a$ of residue $Asp_9$ is approximately 4.1 (fitted to the shift of its degenerate $\beta CH_2$ protons), and interestingly, the backbone amide of residue $Asn_6$, which shows no solvent protection (temperature shift coefficient 7.9 ppb/K), shifts by 0.49 ppm over the pH range 1.2–5.9, with a p$K_a$ of 4.2, indicating an orientation of the aspartyl carboxyl toward the $Asn_6$ amide (there are small shifts for the $Asn_6$ $\alpha$H and $\beta$H with p$K_a$'s between 4.2 and 4.4). For other indications of turns seen in peptide 1–14, the NOEs defining the turn-like conformations at positions 9–12 and 10–13 are still present in the longer peptide.

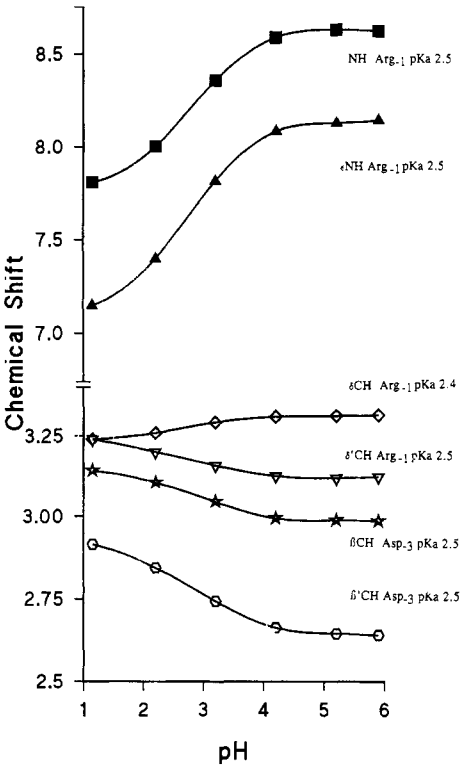


FIGURE 6: pH titration of peptide −9 to 14. The changes in chemical shift of various resonances of residues $Arg_{-1}$ and $Asp_{-3}$ in peptide −9 to 14 with changes in pH are shown. Each resonance shows a change in chemical shift with a p$K_a$ between 2.4 and 2.5.

One particularly unusual feature in the spectrum of peptide −9 to 14 in 50% TFE/50% water was the behavior of $Arg_{-1}$, for which the side-chain $\delta CH_2$ protons were well resolved (0.19 ppm at pH 5.9, 292 K), indicating different magnetic environments for these protons and hence a restricted side-chain rotation. It was observed that the separation of these protons was lost at lower pH and that the shifts converged with a p$K_a$ of 2.4–2.5 (Figure 6; the collapse of the separation of the $Arg_{-1}$ $\delta CH_2$ protons was reversed by increasing the pH). In addition, there were large changes in the shifts of the backbone NH and side-chain $\epsilon$NH protons of residue $Arg_{-1}$, again with a p$K_a$ of 2.5. The p$K_a$ of the residue $Asp_{-3}$ is 2.5 (from $\beta CH_2$ protons), suggesting an interaction between the side chains of residues $Asp_{-3}$ and $Arg_{-1}$. Several factors indicated that this interaction was quite strong. The p$K_a$ for the $Asp_{-3}$ $\beta$-carboxyl is significantly lower than the expected value (around 4; e.g., p$K_a$ of $Asp_9$ = 4.1), as would be expected for a strong interaction with a positively charged species (increased stability of the two charged species). In addition, the resonances of $Arg_{-1}$ were strongly shifted downfield compared with random coil positions, indicating the influence of hydrogen bonding [the shifts of residues $Arg_{-1}$ and $Arg_5$ are $\epsilon$NH 8.14 and 7.21 and NH 8.64 and 7.53 ppm, respectively, and the random coil shifts are $\epsilon$NH 7.17 and NH 8.27 (Wuthrich, 1986); the backbone amide of $Arg_5$ shows an upfield shift associated with a helical conformation], and the NOE $d_{\beta N}(i,i+2)$ $Asp_{-3}$-$Arg_{-1}$ places the side chain of $Asp_{-3}$ close to residue $Arg_{-1}$.

Strong interactions between aspartyl and arginyl side chains are known in proteins (Mitchell et al., 1992), involving both a charge interaction and a pair of hydrogen bonds. Among the features of these charged hydrogen bonds are that they commonly occur at a spacing $i,i+2$ and are found exposed on the protein surface, since the net energy for the interaction between the side chains, consisting of two hydrogen bonds and an ion pair, is more favorable than the interaction of all

Table 1: Sequence Comparisons for Thrombin Receptor[a]

```
                                    50
                                    V
mouse   SER....TDA TVNPRSFFLR NPSENTFELV PLGDEEEEEK NESVLLEGRA VYLNISLPPH
                                    V
  rat   SERMYATPYA TPNPRSFFLR NPSEDTFEQF PLGD..EEEK NESIPLEGRA VYLNKSRFPP
                                    V
crilo   SEM....TDA TVNPRSFFLR NPGENTFELI PLGD..EEEK NESTLPEGRA IYLNKSHSP.
                                    V
human   SK....ATNA TLDPRSFLLR NPNDK.YEPF ....WEDEEK NESGLTEYRL VSINKSSPLQ

                          45                    65

Hirudin variant I       TPKPQ SHNDGDFEEI PEEYLQ-COO⁻
```

[a] An alignment of several sequences of thrombin receptor from around the thrombin cleavage site is shown (the cleavage site is indicated with an arrow). The sources are (1) *Musculus musculus* (mouse), S. R. Coughlin, submitted to EMBL data bank, 1992, (2) *Rattus norvegicus* (rat), Zhong et al. (1992), (3) *Cricetulus longicaudatus* (Chinese long-tailed hamster), Rasmussen et al. (1991), and (4) *Homo sapiens*, Vu et al. (1991a). An alignment with the sequence at the C-terminal section of hirudin is also shown.

the groups with water. It is apparent that an interaction of this type will no longer be viable at low pH where the charge on the aspartyl is reduced, and the energetically favored situation will be the interaction of these groups with the solvent water. The conformation about these residues is defined by the NOEs and has the characteristics of the "side-on" interaction described by Mitchell et al. (1992), in which the distal nitrogens on the arginine side chain are exposed on the surface while the $\epsilon$NH is buried. This is the geometrically favored conformation for $i,i+2$ interactions, and our evidence suggests that the hydrogen-bonding pattern is very similar to that seen for the surface residues $D_{180}PR_{182}$ in human carbonic anhydrase, where the carboxyl oxygens are involved in bifurcated hydrogen bonds with the backbone amide and side-chain $\epsilon$NH and terminal $\eta$NH groups of arginine (residue $P_{181}$ is the first residue in a short helix; e.g., PDB entry 1CA2; Eriksson et al., 1988). In water alone, the $Arg_{-1}$ $\delta CH_2$'s were only slightly separated (0.05 ppm; no resolution of the $\delta CH_2$ protons of $Arg_5$ was seen under any conditions), so although this interaction was still present to some extent, it is clear that the promotion of intrapeptide hydrogen bonding by the TFE/water mixture was responsible for the ability to observe the interaction (both a direct effect on the interaction itself and indirectly by stabilizing the backbone conformation of the peptide in this area so the interacting groups can be placed close to each other in a stable fashion).

## DISCUSSION

In peptide 1–14 the principal structural elements are two overlapping turns, 5–8, and 6–9 (type I), the second certainly stabilized by a hydrogen bond $6_{CO}$–$9_{NH}$. Reference to the table of thrombin receptor sequences (Table 1) indicates that there are differences between the human, rat, mouse, and hamster proteins, but none which would be expected to have a serious consequence for this observed structure. Residue $Asn_8$ is replaced by either Ser or Gly, both of which are common in reverse turns (the serine side chain is small and has hydrogen-bonding potential for interaction with $i+2$ backbone groups, and glycine is small and may adopt any backbone conformation and is particularly common at residue 4 in the type I and II turns). The replacement of $Asp_9$ with glutamic acid may have some steric consequence (since it is a larger residue), but the interaction of the negatively charged side chain with the backbone amide of residue $Asn_6$ need not be disrupted. The more tenuous populations of overlapping turns indicated for residues 9–12 and 10–13 do, however, correspond to an area of considerable sequence variation. The alternative residues present for $Lys_{10}$ and $Pro_{13}$ are hardly conservative replacements, and the residue Thr is inserted between positions 10 and 11. It is not clear what consequences these changes would have, but the insertion of Thr will certainly serve to further separate the two structural elements 5–9 and 9–13. It may be significant that the most strongly formed structural elements correspond to the more highly conserved sequence.

In the longer peptide –9 to 14, which contains the thrombin cleavage site, the striking structural properties are, first, the helix encompassing the cleavage site and, second, the involvement of the $Arg_{-1}$ residue in a charged hydrogen bond with $Asp_{-3}$. The sequence $Pro_{-2}$ to $Arg_5$ is very highly conserved in the four thrombin receptor sequences shown in Table 1. Since this appears to be a self-contained structural element, it would be surprising if there were any significant differences in the structure of this region between proteins from different species. The substitution of the human $Leu_3$ by Phe in the other proteins probably does little to disrupt the helix. Calculations showed that the residue Phe can be accommodated in the volume available for the residue $Leu_3$. There is also a sequence difference at residue –3, with the Asp at this position replaced by Asn in all the nonhuman sequences. Although hydrogen-bonding potential exists in the uncharged Asn, there is no charge component to stabilize the interaction with the Arg side chain observed in peptide –9 to 14, and so it is unlikely that the interaction is significant in these proteins. In the human receptor, it remains likely that the interaction seen for the peptide in the TFE/water mixture will also be present in the protein, where the backbone structure will be relatively rigid and there will be a degree of solvent protection afforded by the remainder of the protein surface (a reduced dielectric constant at the protein surface). It should be noted that the interaction of the Asn side chain with the $i+1$ backbone amide proton ($Arg_{-1}$) *is* expected to be present, since Asp and Asn are interchangeable in this conformation in proteins, at the N-terminus of a helix beginning with a proline residue (MacArthur & Thornton, 1991).

These conclusions have consequences for the interaction of thrombin with the cleavage site on the thrombin receptor. The helical structure must be partially unwound before proteolysis can take place [Hubbard et al. (1993) have recently modeled the unwinding of secondary structure elements at cleavage sites for the serine protease trypsin], and the charged hydrogen bond must likewise be broken, in order that the arginine side chain be able to enter the specificity pocket on the enzyme.

*A Model for the Interaction of the Thrombin Receptor with Thrombin during Activation.* In preliminary modeling calculations we have placed the calculated structure of peptide –9 to 14 into the substrate binding cleft of thrombin (Figure 7), and from this we are able to make certain observations about the mode of binding of the receptor to thrombin.

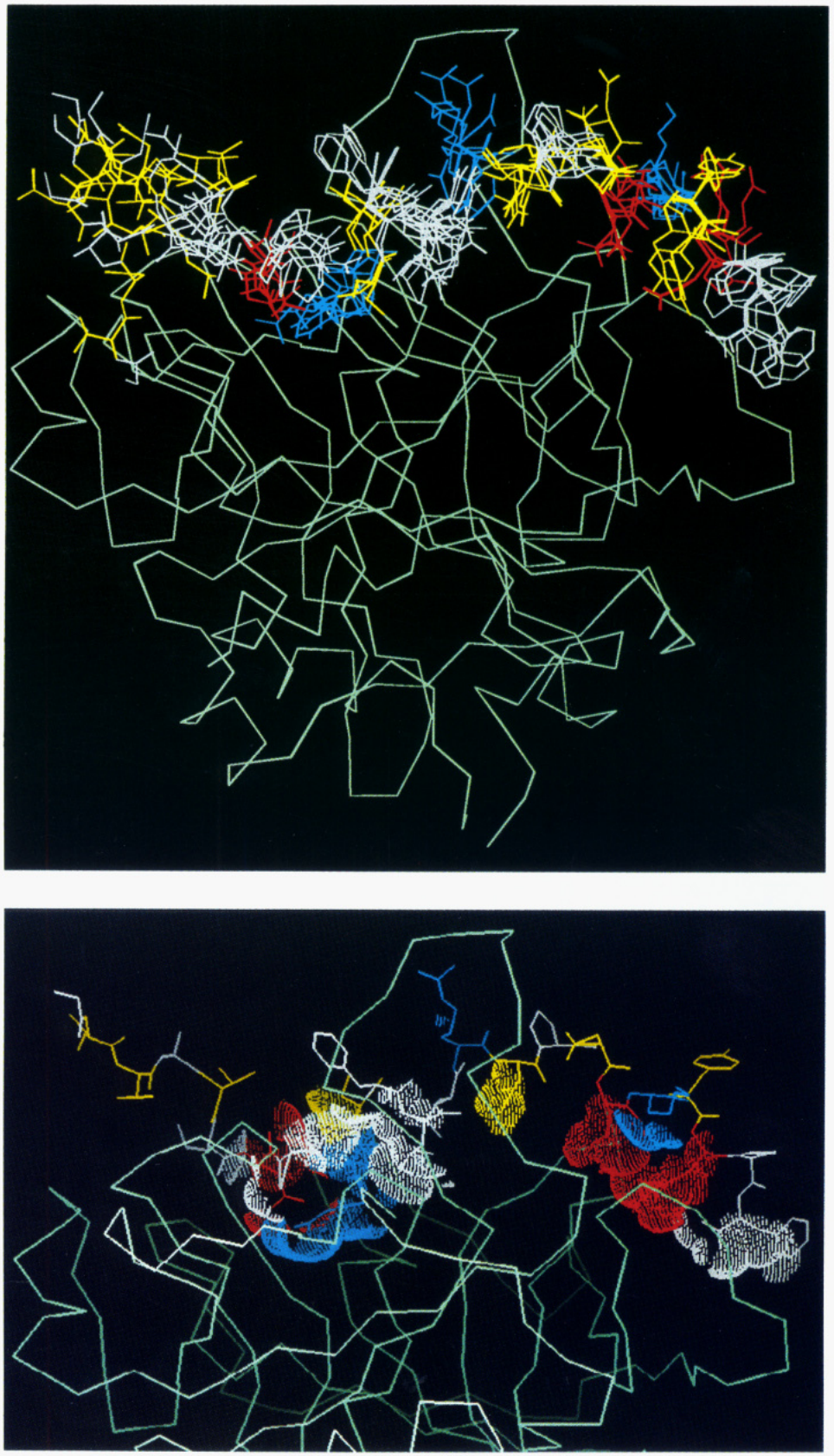

FIGURE 7: Model for the *initial* complex of the 33–55 region of the thrombin receptor (peptide –9 to 14) with thrombin. Both panels show an $\alpha$-carbon trace for thrombin (from the P1DWE PDB entry) in green and peptide –9 to 14 color coded according to polarity of the residue (white = hydrophobic, blue = basic, red = acidic, and yellow = hydrophilic). In the upper panel six of our calculated structures are shown, clustered into the substrate binding cleft. In the lower panel a single structure is shown, together with a dotted contact surface for the peptide with the enzyme (calculated as the excluded surface for a 0.5-Å probe).

The interaction of thrombin with its substrates is generally assumed to follow the two-step mechanism observed for the thrombin–hirudin interaction. In the first step, a positively charged surface patch some distance from the active site, known as the anion-binding (or fibrinogen) exo site, creates a positive field extending into the extramolecular space, which is able to preorient the approaching substrate by virtue of an ionic interaction with a negatively charged patch which lies

near the C-terminus of hirudin. The binding of these two areas therefore leads to the rapid formation of a productive complex, in which much of the binding energy is actually contributed by the formation of intimate complementary hydrophobic contacts at the exo site. In the thrombin receptor, the principal site of interaction with the exo site can be placed in the region $K_{10}YEPF_{14}$, since this shows some homology to the sequence $D_{55}FEEL_{59}$ of hirudin which binds to the exo site and because synthetic peptides corresponding to residues 12–29 of the thrombin receptor are known to displace hirudin by competing at the exo site (Liu et al., 1991). This region of hirudin exists in an extended conformation in the complex with thrombin, and while in our calculated structure for the peptides the corresponding region shows indications of a turn-like conformation, it is quite possible, as discussed above, that the NOE contacts here defining a turn arise as a result of averaging between several more extended conformations. In any case, during the formation of hydrophobic contacts as this region binds to thrombin (in a fashion analogous to hirudin), it is likely that an approximately extended conformation is adopted.

In the second step of the interaction between thrombin and hirudin, the N-terminal portion in hirudin binds over the entrance to the active site. In substrates or other inhibitors such as PPACK, an arginine residue enters the specificity pocket and hydrogen bonds to an aspartyl residue at the base of the pocket ($Asp_{189}$), while other residues close in the sequence to this arginine interact with various other sites placed around the entrance to the specificity pocket. Cleavage of the bound substrate then proceeds on the C-terminal side of the arginine. In the case of the thrombin receptor, our calculations indicate that the length of peptide −9 to 14 is approximately correct such that it places the residue $Arg_{-1}$ at the entrance to the specificity pocket and that the residues $Leu_{-4}$ and $Pro_{-2}$ interact with the apolar pocket and P2 site on thrombin, respectively (as found in preliminary reports of the crystal structure of the thrombin receptor peptide complexed with thrombin; Stubbs & Bode, 1993). However, in the thrombin receptor, there must be an additional step between binding at the active site and cleavage, since the N-terminal section of the helical structure around the cleavage site must be unwound into a more extended conformation, and additionally in humans and $Asp_{-3}/Arg_{-1}$ interaction broken to free the arginine side chain, before cleavage can occur. Examination of the model for the initial complex reveals that, during the cleavage reaction, as the hydrogen bond between residue $Asp_{-3}/Arg_{-1}$ is broken, and the arginine side chain moves into the specificity pocket, then the local backbone conformation around residue $Arg_{-1}$ must become more extended in order to accommodate these movements.

In addition to the features of the bound structure of the thrombin receptor predicted above, we found that the peptide only fitted well into the substrate cleft on the enzyme when there was a slight bulging of the peptide away from the enzyme, so that the contact with thrombin was smallest at residues $Arg_5$, $Pro_7$, and $Asn_8$ [all other residues were involved in extensive contacts, except at the N-terminus of the peptide where, in accordance with the TrNOE data of Ni et al. (1992), we find that there are few contacts; the contact surface is illustrated in Figure 7]. The bending of the peptide required to achieve this is centered at residues $Asp_9$ and $Lys_{10}$, which may be an artifact, since these residues are the least well-defined by the NOEs in this region (the positions in space of either end of the peptide are defined by the requirement to bind at the exo site and active site, and the bending occurs in order to fit to these positions). It is interesting to note that this region has an ill-defined structure, possibly indicating weak binding in the crystal structure (Stubbs & Bode, 1993).

Turning to the implications of these structural components for the function of the thrombin receptor, we propose that they aid in the regulation of the activation of the system. It is well established that thrombin, with its many biological functions, is carefully regulated at several levels (activation by cleavage of prothrombin; multiple binding sites for different macromolecular ligands; narrow substrate specificity arising as a result of the steric hindrance of entry of potential substrates to the active site). In addition, it is known that some substrates for thrombin form part of the regulation process by "protecting" themselves against cleavage. For example, in protein C, two aspartyl residues at position −3 and +3 make protein C a poor substrate for thrombin because of a charge conflict in the binding sites for these residues with glutamyl residues in thrombin ($Glu_{39}$ and $Glu_{192}$; Stubbs & Bode, 1993). However, when thrombin binds thrombomodulin, structural changes circumvent these charge conflicts, and the cleavage of protein C proceeds easily. In a similar fashion, with the thrombin receptor, there are several features which would contribute to substrate-level control of the activation. First, as with protein C, regulation is achieved by making the receptor a relatively poor substrate for thrombin. Hence, like protein C there is an aspartyl at position −3, and there is leucine at position −4 which makes contact with a binding site best suited to aromatic residues, and positions 2, 3, and 4 have large residues which have difficulty fitting into their contact pockets on the thrombin surface and hence reduce binding efficiency (Stubbs & Bode, 1993). In addition to these sequence conflicts with an ideal thrombin cleavage site, the poor binding between residues 1 and 10 observed in the crystal structure (Stubbs & Bode, 1993) is likely to arise from the series of turns formed in the unbound substrate between residues 5 and 9, which we have described above, that may tend to oppose complex formation. In a fashion equivalent to the structural change promoted by thrombomodulin in protein C, in the thrombin receptor there must be a partial unwinding of the helical structure around the cleavage site. This may serve to make the thrombin receptor absolutely specific to thrombin in order to avoid inappropriate activation by other circulating serine proteases.

The data presented also reveal something about the interaction of the newly exposed N-terminus with the remainder of the thrombin receptor as a tethered ligand. The destruction of the self-contained helical unit between residues −2 and 5 during activation of the receptor leads to the loss of helical structure in this region, as confirmed by the observation that the region $S_1FLLR_5$ in peptide 1–14 was unstructured. This appears to exclude the possibility that the conformation adopted by this region at the binding site for the tethered ligand is helical and hence suggests that it binds in a more extended conformation. Since the tethered ligand is present at high concentrations in the thrombin receptor prior to activation, albeit "blocked" by an N-terminal 42-residue segment, it may be important to eliminate the possibility of inappropriate activation by winding up the sequence into helix, thereby "hiding" the conformation which is able to activate the receptor. The more obvious steric hindrance of access of the binding site by the N-terminal extension may not be a sufficient means of downregulation of the activation of the thrombin receptor, and so more subtle structural elements are needed.

## ACKNOWLEDGMENT

We thank Dr. J. Fox for peptide synthesis, Dr. M. Osborne for X-ray microanalysis, and Mr. A. J. Pemberton for maintaining the NMR and computer facilities.

## REFERENCES


Baker, E. N., & Hubbard, R. E. (1984) *Prog. Biophys. Mol. Biol. 44*, 79–179.

Banner, D. W., & Hadvary, P. (1991) *J. Biol. Chem. 266*, 20085–20093.

Bar-Shavit, R., Kahn, A., Wilner, G. D., & Fenton, J. W. (1983) *Science 220*, 728–731.

Berliner, L. J., Ed. (1992) *Thrombin: Structure and Function*, Plenum Press, New York.

Berndt, M. C., & Phillips, D. R. (1981) in *Platelets & Pathology* (Gordon, J. L., Ed.) pp 43–74, Elsevier/North-Holland Biomedical Press, Amsterdam.

Brooks, B. R., Bruccolei, R. E., Olafson, B. D., States, D. J., Swaminathan, S., & Karplus, M. (1983) *J. Comput. Chem. 4*, 187–217.

Brünger, A. T. (1992a) *XPLOR 3.1*, President and Fellows of Harvard University, Cambridge, MA.

Brünger, A. T. (1992b) *XPLOR Version 3.1. A System for X-ray Crystallography and NMR*, Yale University Press, New Haven, CT.

Buck, M., Radford, S. E., & Dobson, C. M. (1993) *Biochemistry 32*, 669–678.

Cann, J. R., London, R. E., Unkefer, C. J., Vavrek, R. J., & Stewart, J. M. (1987) *Int. J. Pept. Protein Res. 29*, 486–496.

Chen, L. B., & Buchanan, J. M. (1975) *Proc. Natl. Acad. Sci. U.S.A. 72*, 131–135.

Coller, B. S., Ward, P., Ceruso, M., Scudder, L. E., Springer, K., Kutok, J., & Prestwich, G. D. (1992) *Biochemistry 31*, 11713–11720.

Dyson, H. J., Rance, M., Houghten, R. A., Lerner, R. A., & Wright, P. E. (1988) *J. Mol. Biol. 201*, 161–200.

Dyson, H. J., Mertuka, G., Waltho, J. P., Lerner, R. A., & Wright, P. E. (1992) *J. Mol. Biol. 226*, 795–817.

Eriksson, A. E., Jones, T. A., & Liljas, A. (1988) *Proteins: Struct., Funct., Genet. 4*, 274–282.

Grabham, P. W., Grand, R. J. A., Byrd, P. J., & Gallimore, P. H. (1988) *Exp. Eye Res. 47*, 123–133.

Grand, R. J. A., Grabham, P. W., Gallimore, M. J., & Gallimore, P. H. (1989) *EMBO J. 8*, 2209–2215.

Gurwitz, D., & Cunningham, D. D. (1988) *Proc. Natl. Acad. Sci. U.S.A. 85*, 3440–3444.

Hubbard, S. J., Thornton, J. M., & Campbell, S. F. (1992) *Faraday Discuss. Chem. Soc. 93*, 13–23.

Jaeger, E., Remmer, H. A., Jung, G., Metzger, J., Oberthür, W., Rücknagel, K. P., Schäfer, W., Sonnenbichler, J., & Zetl, I. (1993) *Biol. Chem. Hoppe-Seyler 374*, 349–362.

Jalink, K., & Moolenaar, W. H. (1992) *J. Cell Biol. 118*, 411–419.

Karle, I. L., Flipper-Anderson, J. L., Uma, K., Balaram, H., & Balaram, P. (1989) *Proc. Natl. Acad. Sci. U.S.A. 86*, 765–769.

Lau, S. Y., Taneja, A. K., & Hodges, R. S. (1984) *J. Chromatogr. 317*, 129–140.

Liu, L. W., Vu, T.-K. H., Esmon, C. T., & Coughlin, S. R. (1991) *J. Biol. Chem. 266*, 16977–16980.

Llinas, M., & Klein, M. P. (1975) *J. Am. Chem. Soc. 97*, 4731–4737.

MacArthur, M. W., & Thornton, J. M. (1991) *J. Mol. Biol. 218*, 397–412.

Means, E. D., & Anderson, D. K. (1986) *Ann. N.Y. Acad. Sci. 485*, 314–322.

Mitchell, J. B. O., Thornton, J. M., Singh, J., & Price, S. L. (1992) *J. Mol. Biol. 226*, 251–262.

Nelson, J. W., & Kallenbach, N. R. (1986) *Proteins 1*, 211–217.

Nelson, J. W., & Kallenbach, N. R. (1989) *Biochemistry 28*, 5256–5261.

Ni, F., Ripoll, D. R., Martin, P. D., & Edwards, B. F. P. (1992) *Biochemistry 31*, 11551–11557.

Nilges, M. N., Clore, G. M., & Gronenborn, A. M. (1988a) *FEBS Lett. 229*, 317–324.

Nilges, M. N., Clore, G. M., & Gronenborn, A. M. (1988b) *FEBS Lett. 239*, 129–136.

Rasmussen, U. B., Vouret-Craviari, V., Jallat, S., Schlesinger, Y., Pages, G., Pavirani, A., Lecocq, J. P., Pouyssegur, J., & Van Obberghen-Schilling, E. (1991) *FEBS Lett. 288*, 123–128.

Richardson, J. (1981) *Adv. Protein Chem. 34*, 167–339.

Richardson, J. S., & Richardson, D. C. (1988) *Science 240*, 1648–1652.

Richardson, J. S., & Richardson, D. C. (1989) in *Prediction of Protein Structure and Principles of Protein Conformation* (Fasman, G., Ed.) Plenum Press, New York.

Sabo, T., Gurwitz, D., Motola, L., Brodt, P., Barak, R., & Elhanaty, E. (1992) *Biochem. Biophys. Res. Commun. 188*, 604–610.

Scarborough, R. M., Naughton, M. A., Teng, W., Hung, D. T., Rose, J., Vu, T.-K. H., Wheaton, V. I., Turck, C. W., & Coughlin, S. R. (1992) *J. Biol. Chem. 267*, 13146–13149.

Shuman, M. A. (1986) *Ann. N.Y. Acad. Sci. 485*, 228–239.

Siligardi, G., Drakes, A. F., Mascagni, P., Neri, P., Lozzi, L., Niccolai, N., & Gibbons, W. A. (1987) *Biochem. Biophys. Res. Commun. 143*, 1005–1011.

Snider, R. M. (1986) *Ann. N.Y. Acad. Sci. 485*, 310–313.

Stubbs, M. T., & Bode, W. (1993) *Thromb. Res. 69*, 1–58.

Suidan, H. S., Stone, S. R., Hemmings, B. A., & Monard, D. (1992) *Neuron 8*, 363–375.

Tirado-Rives, J., & Jorgensen, W. L. (1991) *Biochemistry 30*, 3864–3871.

Van Obberghen-Schilling, E., Rasmussen, U. B., Vouret-Craviari, V., Lentes, K.-U., Pavirani, A., & Pouyssegur, J. (1993) *Biochem. J. 292*, 667–671.

Vassallo, R. R., Kieber-Emmons, T., Cichowski, K., & Brass, L. F. (1992) *J. Biol. Chem. 267*, 6081–6085.

Vu, T.-K. H., Hung, D. T., Wheaton, V. I., & Coughlin, S. R. (1991a) *Cell 64*, 1057–1068.

Vu, T.-K. H., Wheaton, V. I., Hung, D. T., Charo, I., & Coughlin, S. R. (1991b) *Nature 353*, 647–677.

Walz, D. A., Fenton, J. W., & Shuman, M. A. (1986) *Ann. N.Y. Acad. Sci. 485*.

Zhong, C., Hayzer, D. J., Corson, M. A., & Runge, M. S. (1992) *J. Biol. Chem. 267*, 16975–16979.